



## NONLINEAR FIBER-BASED ANALYSIS OF RECTANGULAR CONCRETE WALLS DESIGNED WITH DIFFERENT ANCHORAGE DETAILS

Sriram Aaleti<sup>1</sup> and Sri Sritharan<sup>2</sup>

### ABSTRACT

Structural walls are frequently used in buildings to resist earthquake lateral loads because of their effectiveness in limiting the building drifts and minimizing damage to both structural and non-structural elements. In a recent PreNEESR collaborative project, large-scale cyclic testing of three rectangular concrete structural walls with different anchorage details was conducted at the Multi-Axial Subassemblage Testing (MAST) facility at the University of Minnesota. All three walls had two different stiffness and strength in the two in-plane loading directions as they were modeled to represent the response of a T-shaped concrete wall. These walls were identical except for the fact that the longitudinal reinforcement was anchored into the foundation without any splices, couplers and conventional lap splices, respectively. The fiber-based nonlinear beam-column element available in OpenSees software was used to model the walls with adequate attention to capture the influence of different anchorage details. In addition to capturing the total global response, the accuracy of the analysis was also examined in terms of simulating the local response as well as various displacement components due to flexure, bond slip at the critical section resulting from strain penetration, and shear. A zero-length bond slip element was used to account for the strain penetration effects while a nonlinear spring element was used to account for the shear deformation. By comparing with the experimental results, it was found that the analytical models well simulated the force-displacement responses including the unloading and reloading stiffness. Various displacement components were well captured. In addition to presenting the analytical models and comparisons of experimental and analysis results, this paper identifies the improvements needed for fiber-based analysis of concrete walls in OpenSees.

### Introduction

Concrete structural walls provide a cost effective way to resist lateral loads and thus they are frequently incorporated as the primary lateral load resisting system in buildings in seismic regions. Structural walls have a high in-plane stiffness, which helps decreasing the structural damage by limiting the inter-story drift during seismic events. The superior performance of the buildings consisted of structural walls as the primary lateral loading system is well documented

---

<sup>1</sup> Graduate Research Assistant, Dept. of Civil, Constr. & Env. Engineering, Iowa State University, Ames, IA 50011

<sup>2</sup>Wilson Engineering Associate Professor, Dept. of Civil, Constr. & Env. Engineering, Iowa State University, Ames, IA 50011

in the literature. Concrete walls can be constructed in different shapes, such as rectangular, T-, L- or C-shaped walls. However, the rectangular walls are more prevalent compared to other shaped walls due to ease of construction and ease of placement of walls along the perimeter of a building. Furthermore, it is common practice to splice the longitudinal reinforcement of walls near the base using either lap splices or mechanical couplers to simplify the construction process. Therefore, understanding the lateral load behavior of rectangular walls with different anchorage details is important for ensuring good structural performance under earthquake loading. With the added emphasis on performance-based design in recent times, it is important to realize that in addition to predicting the global wall response, their local responses need to be adequately quantified by addressing the influence of anchorage details.

This paper presents the approach used for modeling the concrete walls using an open source finite element program OpenSees (Mazzoni et al., 2006) using fiber-based beam-column elements. The results obtained from the experimental investigation are compared with the analysis results to examine the accuracy of the OpenSees models.

### Description of Test Walls

The rectangular concrete walls were designed to replicate the web direction response of a 50% scale prototype T-wall designed for a six story building located in Los Angeles, CA. The details of the prototype T-wall and the six-story prototype building are presented in Brueggen *et al.* (2009). The reinforcement in the rectangular walls was designed to ensure that the flexural strain gradient along the wall height and the inelastic curvature at the base will be comparable to those of the T-wall in the flange-in-tension and flange-in-compression direction loading along the web. This design requirement caused the rectangular walls to have unsymmetrical amounts and distribution of longitudinal steel in the boundary elements. Complete details about the design considerations adopted for the rectangular walls can be found in Johnson (2007).

The first wall specimen used continuous longitudinal reinforcement from the footing to the top of the wall without any splices, which was identified as RWN (where “RW” represented rectangular wall while “N” referred to no splicing). The second wall specimen used mechanical couplers to splice the longitudinal reinforcement near the wall-to-foundation interface, which was referred to as RWC (where “C” represented couplers). The third wall specimen used conventional lap splices near the wall-to-foundation interface, which was identified as RWS (where “S” referred to splices).

Figure 1 presents the cross-section details of the three rectangular walls. All three walls were 254 in. tall, 90 in. long and 6 in. thick. The walls contained two different boundary elements: one with #6 ( $d_b = 0.75$  in., where  $d_b$  is the bar diameter) and #5 ( $d_b = 0.625$  in.) longitudinal bars, the other with #9 ( $d_b = 1.125$  in.) longitudinal bars. Consequently, the two boundary elements were referred to as No. 6 boundary element and No. 9 boundary element respectively. Between the two boundary elements, #4 ( $d_b = 0.5$  in.) longitudinal bars were distributed at 18 in. of spacing. All the walls were designed adequately for shear according to ACI 318-02 design code. In accordance with the ACI 318-02, Type-2 mechanical couplers and Class B lap splices were used for splicing the longitudinal reinforcement in RWC and RWS, respectively.

The rectangular walls were subjected to reverse cyclic displacements, applied at 20 ft from the foundation-to-wall interface under displacement control. The applied displacement history for the walls is shown in Figure 1d.

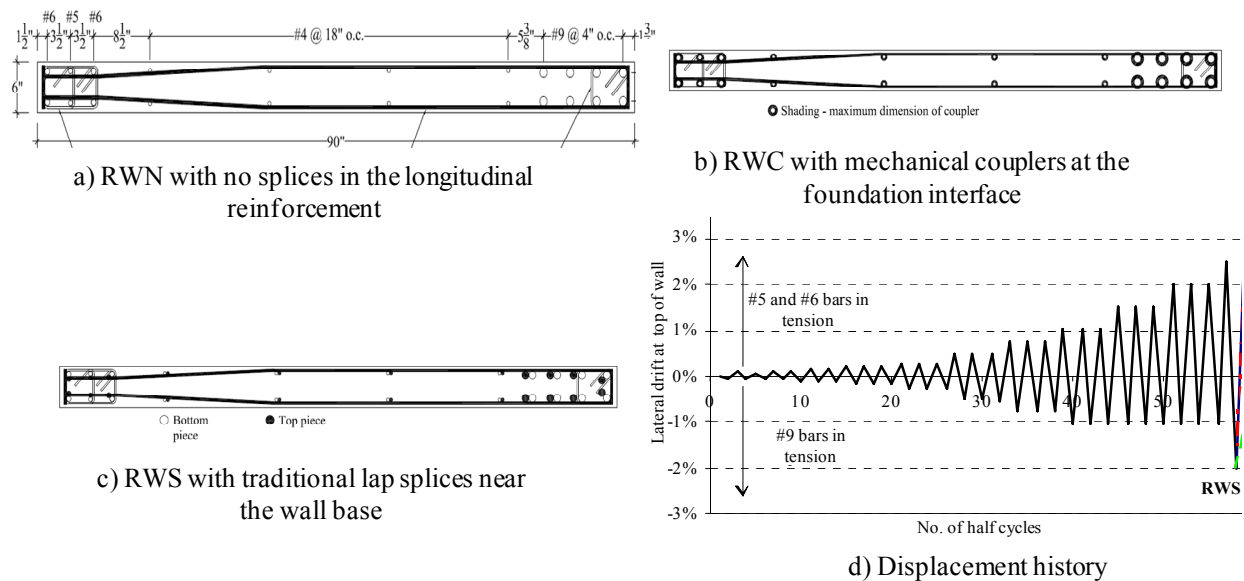


Figure 1 Reinforcement and the applied displacement history details of the three rectangular walls.

### Analytical models

The force-displacement behavior of a structural wall depends on the ratio of the wall height to wall length, which defines the wall aspect ratio. When the aspect ratio is greater than 2.0, the walls are classified as “slender walls” and the flexural deformation is considered to be the prominent contributor to their lateral displacements. However, it is important to note that well designed structural walls undergo several deformation modes when subjected to lateral loads, including flexural deformation mode, shear deformation mode, and deformation due to strain penetration in the form of rotation at the wall base. In order to capture the overall and local responses of concrete walls accurately, an analytical model should capture each of the aforementioned deformation components satisfactorily.

The analytical models to predict the lateral load behavior of the three rectangular walls were developed using fiber based beam-column elements available in OpenSees (OpenSees 2007). The walls were modeled using nonlinear forced-based beam-column elements as these elements have been shown to better capture the spread of plasticity along the length of a member. Described below are the details of the analytical models developed for the three rectangular walls, which include information on how various anchorage details of the test specimens were modeled.

The base block of each wall was rigidly connected to the strong floor. Lateral movement and rotation of the base block with respect to the strong floor were assumed to be negligible. The experimental measurements confirmed this assumption. The base block was represented by a node (i.e., node 1 in Figure 2) in the analytical model and its degrees of freedom were restrained in all the directions. Furthermore, since adequate anchorage was provided for the longitudinal reinforcement in the foundation, the longitudinal bars were assumed to experience no slip in the foundation due to poor anchorage condition.

## Model for RWN

Figure 2a presents a schematic of the fiber-based OpenSees model developed for RWN, which consists of five force-based beam-column elements along the height of the wall. Previous research has shown that sufficiently anchored longitudinal reinforcement of the flexural members experiences slip along a portion of the bar embedment due to strain penetrating along the longitudinal reinforcing bars anchored into a connecting concrete member. It was also demonstrated by Sritharan et al. (2000) and Zhao & Sritharan (2007) that ignoring the strain penetration effects in analytical models will grossly affect the prediction of the local response parameters. Consequently, as recommended by Zhao & Sritharan (2007), a zero-length fiber-based element was used at the interface between the wall and foundation to account for the strain penetration effects. This zero-length interface element had the same cross section as the rectangular wall (i.e., cross section-1 for RWN shown in Figure 2). The steel fibers of this zero-length section were modeled using the strain penetration material model, which correlated the stress in a fully anchored reinforcement with the total slip of the bar at the interface.

Except for the second story, a single force-based beam-column element (i.e., `nonlinearBeamColumn` in OpenSees) with five integration points along its length modeled each story of RWN. The location of integration points followed the Gauss-Lobatto scheme. For example, in an element with five integration points, the integration points were located at both ends of the element (-1.0 and 1.0 in an isoparametric formulation, at the center of the element (0.0 in an isoparametric formulation), and at points located at a distance of 0.17267 times the length of the element from both ends (-0.65465367, 0, 0.65465367) of the element. The second panel was modeled with two force-based elements since the boundary elements were extended 21 in. into the second panel, changing the cross section details at 90 in. from the wall base. A fiber section was used to represent the cross section of the wall. The details of the fiber sections used for the nonlinear beam-column elements are shown in Figure 2a. The wall cross sections in the confined and unconfined regions were discretized using fibers of approximately 0.2 in. x 0.2 in. The confined and unconfined concrete fibers were modeled to follow the Chang and Mander confinement model (1994) with modifications introduced by Waugh (2009) (i.e., `Concrete07` in OpenSees). The average concrete strength in RWN was 7870 psi for the bottom two panels and 6880 psi for the remainder of the wall. The concrete strength was different between the top two and bottom two panels because the wall was cast in two stages. The concrete tensile strength was taken as  $6\sqrt{f'_c}$  (psi) in both cases. However, the tensile strength in the No. 6 boundary region of the first panel was reduced to  $3\sqrt{f'_c}$  (psi) to account for the effects of limited pre-existing shrinkage cracks in the region near the wall base. The concrete young's modulus was approximated to  $57000\sqrt{f'_c}$  (psi). The confined concrete properties in the boundary regions were obtained using the confined concrete model proposed by Mander et al. (1988) based on the details of the transverse reinforcement.

All longitudinal reinforcement (i.e., #4, #5, #6 and #9 bars) was modeled using the `ReinforcingSteel` material model available in OpenSees. This model has the ability to closely follow the strain response of Grade 60 mild steel reinforcement, especially under cyclic loading. The #4 reinforcing bar was modeled using the modified Menegotto-Pinto model (i.e., `Steel02` in OpenSees) because the uniaxial testing of #4 rebar did not exhibit any yield plateau. Furthermore, the strain demand in #4 bars was never reported to exceed 0.035 in/in. The reinforcement properties used for the OpenSees model of RWN are shown in Table 1.

Table 1 Reinforcement properties used in the RWN model based mainly on experimental testing.

Bar size (dia (in.))	Yield Strength (ksi)	Elastic Modulus (ksi)	Tangent at initial strain hardening (ksi)	Strain hardening strain (in/in)	Ultimate strength (ksi)	Strain at ultimate strength (in/in)
#9 (1.125 in.)	66.74	26546	775	0.0086	90.0	0.10
#6 (0.75 in.)	71.00	28249	800	0.0096	96.5	0.10
#5 (0.625 in.)	71.03	28560	875	0.0095	97.5	0.10
#4 (0.5 in.)	58.00	22282	-	-	90.0	0.10
#3 (0.375 in.)	66.00*	29000*	-	-	-	0.12
#2 (0.25 in.)	79.34	29000*	-	-	96.3	0.12

\* assumed

Significant contribution of shear deformations towards the lateral deformation of walls and the existence of shear-flexural coupling in the plastic hinge regions was demonstrated by experimental research on flexural dominant rectangular concrete walls with aspect ratios greater than 2.0 (Thomsen and Wallace 1995; Johnson 2007). Therefore, it follows that to accurately capture the lateral load behavior, it is necessary to account for the shear deformations along the height of the wall. The force-based beam-column element in OpenSees accounts only for the flexural response while ignoring the effects of shear deformation and possible interaction between flexure and shear mechanisms. Although, there are several formulations recommended in the literature to account for the shear deformations in the force-based beam-column elements (Martinelli 2008), no such technique was available in OpenSees to account for the effects of shear deformation. Therefore, the shear deformations in the analytical model were accounted by aggregating the shear deformations using a uniaxial material model (i.e., *Pinching4* in OpenSees) over the flexural response of the nonlinear beam-column element. Although, the section aggregation method enables the shear deformation to be accounted for, it does not account for the effects of flexure-shear interaction.

### Model for RWC

The overall modeling of RWC followed that of the RWN, but it incorporated a sixth force-based beam-column element. This new element was used to model the region containing the mechanical couplers. Figure 2b presents the schematic of the OpenSees model developed for RWC. It was anticipated that the presence of couplers would modify the strain distribution in the bottom region of the wall. A challenge associated with this modeling was that, the length and the area of the couplers varied based on the size of the rebar. Since the response that subjected the #5 and #6 longitudinal bars in tension experienced severe nonlinearity, the length of this beam-column element representing the coupler region was taken as the average length of the #5 and #6 bar couplers. Concrete and longitudinal reinforcement fibers in RWC were modeled as in RWN, while the couplers were modeled with the increased cross sectional area and the stress-strain behavior the same as the corresponding longitudinal reinforcing bar. Because the couplers were kept above the wall-to-foundation interface in the specimen, reinforcement fibers in the zero-length section at the wall-to-foundation interface were modeled using the reinforcing bar area instead of couplers area. The strain penetration effect and the shear deformations were included

in the same manner as it was done in RWN model. Concrete and longitudinal reinforcement fibers were modeled as described in RWN model. The average panel concrete strength of RWC was 7500 psi for bottom two panels and 9100 psi for the top two panels. The longitudinal reinforcement was modeled with same material properties as those in RWN.

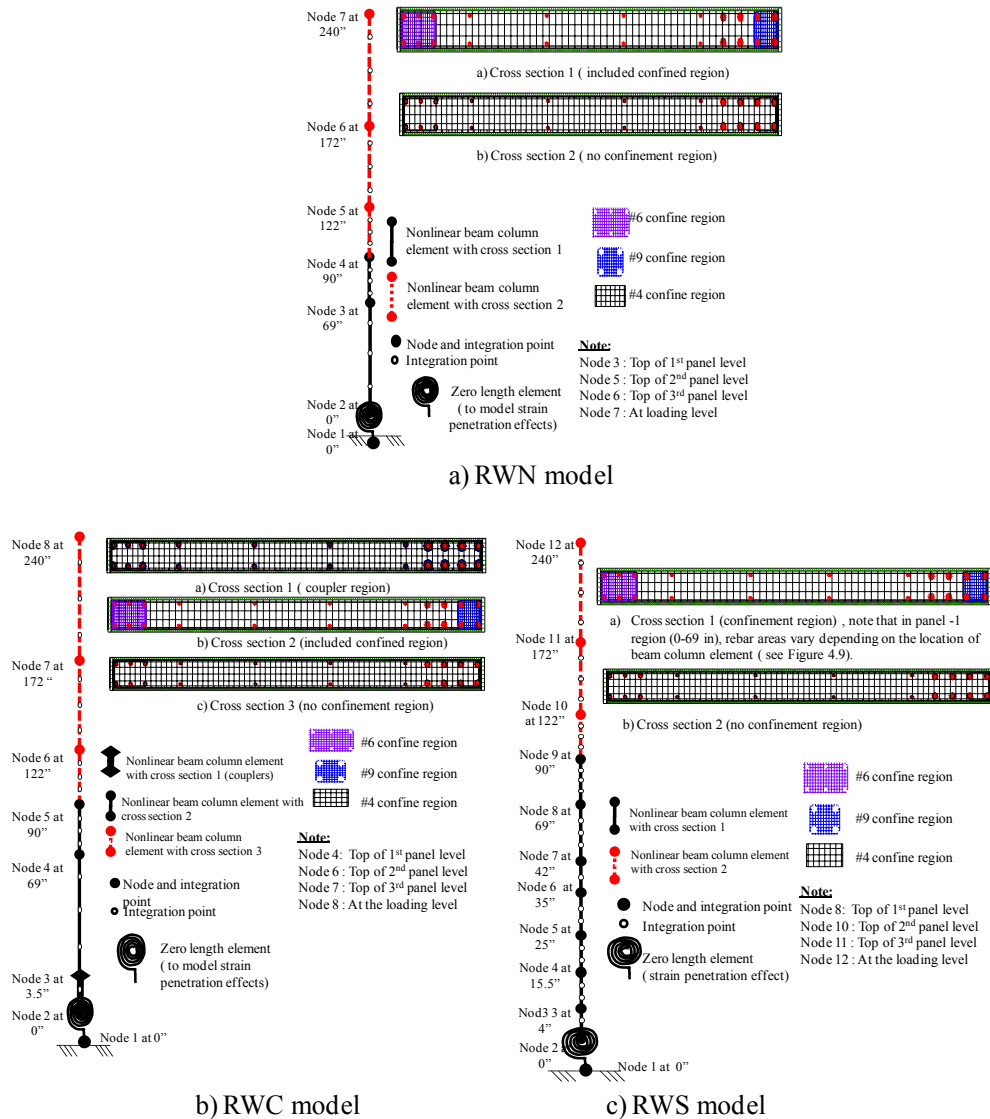


Figure 2 Schematic of the nonlinear fiber-based OpenSees models of the rectangular walls.

### Model for RWS

The overall modeling of RWS was done as for RWN, except for introducing new beam-column elements to model the region containing the traditional lap splices. Figure 2c presents the schematic of the OpenSees model developed for RWS. It is generally accepted that the strength of a spliced bar is almost the same as that of a single embedded bar (Cho and Pincheira, 2006) and therefore lap splices have been typically modeled with a single rebar effectively representing the entire length of the lap splice. However, an analytical model using this assumption underpredicted the lateral load capacity of RWS (Aaleti 2009). Therefore, the lap splice was

modeled using an effective bar with a variable area along the splice length. The effective reinforcing bar areas varied from one bar area to two bar area depending upon the location along the splice. More details about the effective bar area calculation can be found in Waugh et al. (2009) and Aaleti (2009). The lap splice region was modeled using six nonlinear beam-column elements (see Figure 2c) with equivalent longitudinal bar diameters being  $1.0d_b$ ,  $1.5d_b$ ,  $2.0d_b$ ,  $1.5d_b$  and  $1.0d_b$  along the lap splice. The strain penetration effect and the shear deformation in this model were handled in the same manner as in the RWN model. During the test, slip between longitudinal reinforcement, especially the #6 and #5 bars, was observed in lap splice region (Johnson 2007). Since there are neither specific experimental studies nor analytical models found in the literature to model the slip within the spliced region, the potential slip of bars in the spliced region was not modeled.

Concrete and longitudinal reinforcement are modeled as described in RWN model. The average concrete strength for RWS was 8110 psi for bottom two panels and 6580 psi for the top two panels. The longitudinal reinforcement was modeled with same material properties as in RWN.

### Comparison of Experimental and Analytical Results

In this section, the OpenSees analytical results and experimentally observed responses are compared for three rectangular walls and appropriate comments are made. In addition to the global responses, the analytical model was validated by examining the accuracy of the local responses of RWN, including the force-displacement response of RWN at first story level (69 in. from the base of the wall), experimental and calculated contribution of various deformation components to the lateral displacement at the first story level and top of wall.

### Global Cyclic Responses

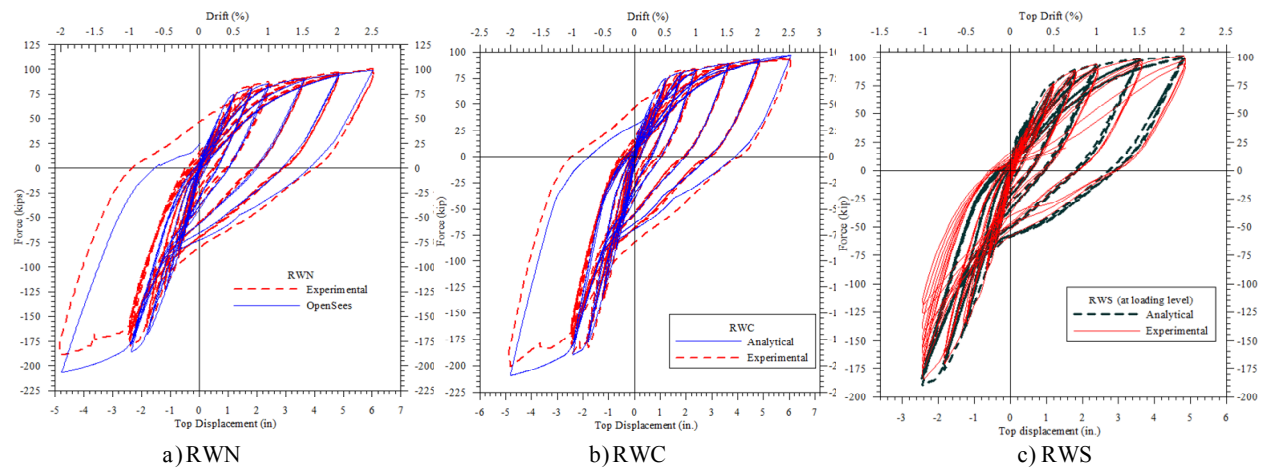


Figure 3 Comparison of measured and calculated force-displacement responses.

The measured and calculated cyclic top lateral displacement responses of RWN, RWC and RWS for the applied displacement history are shown in Figure 3a, 3b and 3c respectively. As seen in this figure, the OpenSees simulation accurately captured the force-displacement responses of the three walls for the loading direction that subjected the #6 and #5 longitudinal

bars in tension. The unloading stiffness, reloading stiffness, and residual displacements were all well simulated by the analysis model up to a lateral displacement of 6.0 in. (i.e., +2.5% drift) in this direction. In the opposite direction, which subjected the #9 bars in tension, the analytical response closely matched the experimental response up to about 2.4 in. of lateral displacement. This was the peak lateral displacement for the majority of testing. However, the agreement is not as good as that observed for the other direction. The calculated peak values for all the three walls were within 3% of the experimental values for up to 2.4 in. (i.e., 1% drift) of lateral displacement in the #9 bars in tension direction. At 4.8 in. of lateral displacement, for #9 bars in tension, the analytical model overestimated the lateral force resistance of the walls by 5% to 7.9%. The overestimation of the load and the underestimation of the residual displacements are due to disregarding of the shear degradation in the OpenSees model, which is further discussed in the next section. The initial stiffness in the both directions was captured with good accuracy. The strength degradation observed in RWS at -1% drift was not captured by the OpenSees model as this was due to the slip of the longitudinal bars in the lap splices during the repeated cyclic loading.

### First Story Cyclic Response of RWN

To ensure that the OpenSees model adequately captured the different deformation components accurately, the response at first story level was examined. The shear deformation contributed a significant amount towards the first story lateral displacement, due to the reduction of the shear stiffness caused by the flexural damage and yielding of the longitudinal reinforcement. Thus, the comparison of lateral load response at the first story provided an opportunity to examine the modeling accuracy of the shear deformation and nonlinear force-based beam-column elements. The calculated and measured force-displacement responses and the shear distortion response of RWN at the first panel level are shown in Figure 4a and Figure 4b respectively.

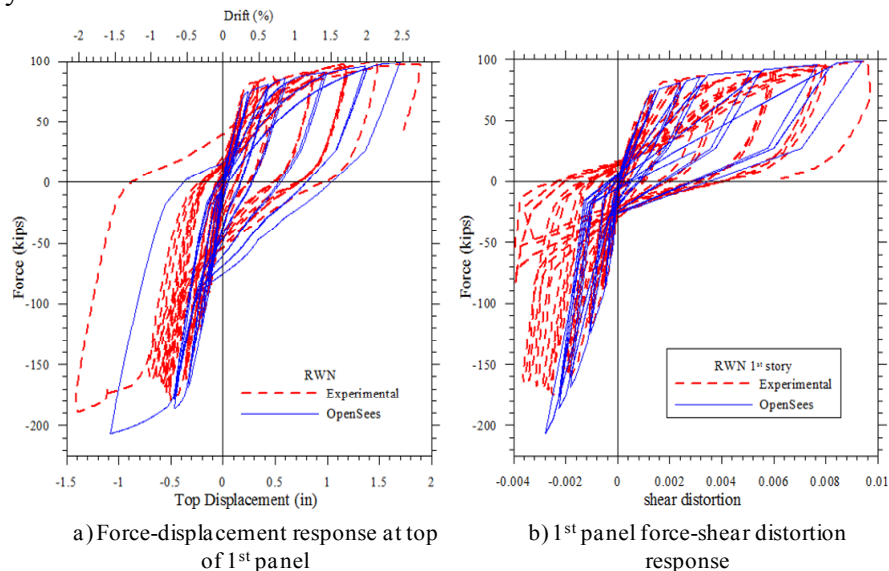


Figure 4 Overall and the shear responses of RWN at the first story level.

OpenSees model did not capture the first story cyclic response in both loading directions as accurately as it did at the top of the wall. The shear model also did not capture the observed



cyclic shear response. The shear response did not account for possible strength degradation and softening of the structure expected due to repeated loading to the same lateral displacement. However, the initial and post-yield stiffnesses and the envelope curves at the first story level were predicted accurately by the OpenSees model.

### Comparison of Deformation Components

Calculated and experimental values of various deformation component responses of RWN at the first story level and the top of the wall during the peak displacements are compared and appropriate comments are presented. Since the #6 and #5 bars in tension direction response was of significant interest, the comparisons are presented for that loading direction only.

The comparison between the calculated and measured values of various deformation components of RWN at the top of the wall and the 1<sup>st</sup> story level are shown in Figure 5a and Figure 5b, respectively. It can be seen from the figures that the analytical model over predicted the localized flexural deformation in the first story, while accurately predicted the overall flexural deformation of RWN. The shear deformation and the deformation due to strain penetration in the first panel and at the top of RWN were well captured by the analytical model.

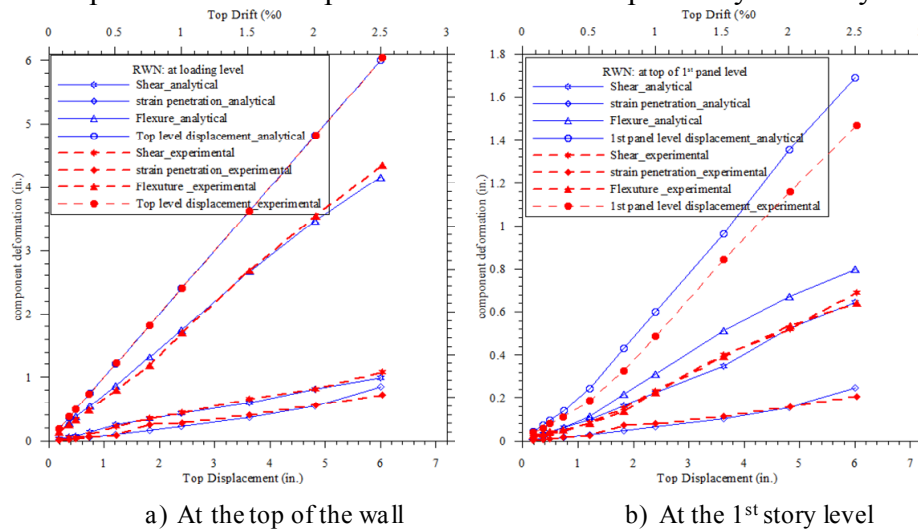


Figure 5 Comparison between the calculated and experimental deformation components at the top and first story level of RWN.

### Conclusions

Three rectangular reinforced concrete walls with different longitudinal reinforcement anchorage details were analyzed using OpenSees with adequate attention given to model the anchorage conditions. The force-based beam-column elements with fiber sections adequately captured the global cyclic force-displacement responses of all the three rectangular walls. The calculated peak forces were within 5% of the experimental values while the loading, unloading and reloading stiffnesses were simulated with good accuracy. For all three rectangular walls, the response in the direction that subjected the #6 and #5 bars in tension was better simulated than the response that subjected the #9 bars in tension. The discrepancy between the experimental and analytical results in the #9 bar in tension direction was caused primarily due to not adequately capturing the shear degradation during the repeated loading to the same lateral displacement in that loading direction. Also, the model did not capture the strength degradation resulted from the

local slip in the splice region. Since the best available approach was used in the analytical simulation, further improvements to the analysis of concrete walls in OpenSees require integration of a new shear as well as a local slip model.

The analytical models captured the various deformation components at the top of the wall with good accuracy. Strain penetration deformation contributed nearly 10% towards the top lateral displacement and was well captured by the analytical model. At the first story level, the analytical models over predicted the flexural deformation at the first panel level by 10 to 40%, depending on the top lateral displacement. At large top lateral displacements, the percentage of error was smaller

### Acknowledgements

The study presented in this paper is based upon the work done as a part of a collaborative PreNEESR project supported by the National Science Foundation (NSF) under Grant No. CMS-0324559. Any opinions, findings, and conclusions expressed in this paper are those of the authors, and do not necessarily represent those of the sponsor.

### References

1. Aaleti, S [2009] "Behavior of rectangular concrete walls under simulated seismic loading", *PhD thesis*, Iowa State University, IA.
2. Brueggen, B. L. [2009] "Performance of T-shaped reinforced concrete shear walls under multi directional loading", *PhD thesis*, University of Minnesota, MN.
3. Cho, J.Y., Pincheira, A. (2006) "Inelastic Analysis of Reinforced Concrete Columns with Short Lap Splices Subjected to Reversed Cyclic Loads", *ACI Structural Journal*, V. 103, No.2, pp 280-290.
4. Chang, G.A., and Mander, J.B. [1994] "Seismic Energy Based Fatigue Damage Analysis of Bridge Columns: Part 1 – Evaluation of Seismic Capacity," NCEER Technical Report No. NCEER-94-0006, State University of New York, Buffalo, NY.
5. Johnson, B. M. "Longitudinal Reinforcement anchorage Detailing effects on RC shear wall Behavior", *Master of Science Thesis*, University of Minnesota, 2007, 391 pp.
6. Mander, J.B., Priestley, M.J.N., and Park, R., [1988] "Theoretical Stress-Strain Model for Confined Concrete," *Journal of Structural Engineering*, American Society of Civil Engineering, Vol. 114, No. 8, August 1988.
7. Mazzoni, S., McKenna, F., Scott, M.H., Fenves, G.L. [2006] "Open System for Earthquake Engineering Simulation," Pacific Earthquake Engineering Research Center, University of California, Berkeley, California, Ver. 1.7.4.
8. Petrangeli, M.; Pinto, P. E., and Ciampi, V., "Fiber Element for Cyclic Bending and Shear of RC Structures, I: Theory," *Journal of Engineering Mechanics*, V. 125, No. 9, 1999, pp. 994-1001.
9. Sritharan, S., Priestley, N., and Seible, F. "Nonlinear Finite Element Analyses Of Concrete Bridge Joint Systems Subjected To Seismic Actions," *Finite Elements in Analysis and Design*. V. 36, 2000, pp. 215-233.
10. Thomsen, J.H., and Wallace, J.W. [1995] "Displacement-Based Design of RC Structural Walls: An Experimental Investigation of Walls with Rectangular and T-Shaped Cross-Sections," Report to the National Science Foundation, Dept. of Civil Engineering, Clarkson University, NY.
11. Waugh J.D, [2009], "Nonlinear Analysis of T-shaped concrete walls subjected to multi-directional displacements", *PhD thesis*, Iowa State University, IA.
12. Zhao, J., and Sritharan, S. [2007] "Modeling of Strain Penetration Effects in Fiber-Based Analysis of Reinforced Concrete Structures," *ACI Structural Journal*, Vol. 104, No. 2, pp. 133-141.